Original Article

Workflow of a Preclinical Robotic Magnetic Resonance Imaging-guided Focused Ultrasound Body System

Nikolas Evripidou[1], Anastasia Antoniou[1], George Lazarou[1], Leonidas Georgiou[2], Antreas Chrysanthou[2], Cleanthis Ioannides[2], Christakis Damianou[1]*

[1]Department of Electrical Engineering, Computer Engineering and Informatics, Cyprus University of Technology, Limassol, Cyprus, [2]Department of Interventional Radiology, German Oncology Center, Limassol, Cyprus

Abstract

Background: Establishing an efficient workflow is crucial for the success of magnetic resonance-guided focused ultrasound (MRgFUS) procedures. The current study provides a comprehensive description of the workflow of a customized MRgFUS robotic body device for preclinical use and accompanied software through experiments in excised porcine tissue. **Methods:** The employed system comprises a single-element spherically focused transducer of 2.6 MHz that can be moved along four PC-controlled axes. A detailed description of essential software functionalities and its integration with a 3T Siemens magnetic resonance imaging (MRI) scanner through Access-I for interactive remote control of the scanner and real-time access to imaging data is provided. Following treatment planning on preoperative MR images, porcine tissue samples were sonicated in rectangular and irregular grid patterns with varying ultrasonic parameters and spatial step under software-based monitoring. **Results:** MRgFUS ablations of *ex vivo* porcine tissue were successfully performed utilizing a multimodal monitoring approach combining MRI-based temperature, thermal dose, and necrotic area mapping, thus demonstrating an efficient procedural workflow. The simulated necrotic regions were in excellent agreement with the actual lesions revealed upon tissue dissection and highly consistent with the planned sonication patterns. The software's ability to accurately identify regions where necrosis did not occur and indicate to the user the specific points to be re-sonicated was demonstrated. **Conclusion:** Overall, the study highlights critical aspects in accurately planning and executing preclinical MRgFUS protocols within an efficient workflow. The provided data could serve as the basis for other researchers in the field.

Keywords: Magnetic resonance-guided focused ultrasound, planning, robotic system, software, ultrasound, workflow

Introduction

Magnetic resonance-guided focused ultrasound (MRgFUS) is a noninvasive treatment modality that uses high-intensity ultrasonic waves to ablate targeted tissue within the body.[1] As a noninvasive modality, it may lead to quicker recovery, lower infection risks, and overall, to a superior life quality compared to standard surgical approaches.[2] Magnetic resonance imaging (MRI) guidance is deemed crucial for the success of FUS ablation since it provides real-time magnetic resonance (MR) thermometry feedback, thereby allowing for the intraprocedural assessment of the therapeutic outcome and adjustment of the sonication protocol as necessary.[1] There are currently two commercial MRgFUS systems for treating body targets, both employing the phased array ultrasonic technology; the first one is the ExAblate 2000/2100 system owned by Insightec (InSightec Inc., Haifa, Israel)[3] and the second one is the Sonalleve system from Profound Medical (Profound Medical Corp., Mississauga, ON, Canada).[4] Both systems have been approved by the US Food and Drug Administration for the treatment of uterine fibroids and pain palliation of bone metastases. They can be integrated into the table of 1.5 and 3 T MRI scanners for a bottom-to-top ultrasonic delivery in prone-positioned patients.

An efficient treatment workflow is critical to the success of MRgFUS procedures since it ensures that patients receive the highest quality of care while minimizing discomfort and risk. It also contributes to efficient time management by optimizing

Received: 26-10-2023 **Revised:** 07-12-2023 **Accepted:** 26-12-2023 **Available Online:** 22-04-2024

Access this article online

Quick Response Code:

Website: https://journals.lww.com/jmut

DOI: 10.4103/jmu.jmu_135_23

Address for correspondence: Dr. Christakis Damianou, Department of Electrical Engineering, Computer Engineering and Informatics, Cyprus University of Technology, 30 Archbishop Kyprianou Street, Limassol 3036, Cyprus.
E-mail: christakis.damianou@cut.ac.cy

How to cite this article: Evripidou N, Antoniou A, Lazarou G, Georgiou L, Chrysanthou A, Ioannides C, *et al*. Workflow of a preclinical robotic magnetic resonance imaging-guided focused ultrasound body system. J Med Ultrasound 2025;33:1-14.

the use of resources (equipment, staff, etc.), potentially improving patient throughput.[5,6] The workflow steps depend on and should be adjusted according to the specifications and unique features of each MRgFUS system. As an example, the ExAblate system performs point-by-point sonications leaving a cooling period between them, whereas a volumetric ablation technique based on a circular sonication pattern progressing from the inside toward the outside is employed by the Sonalleve system.[7] Accordingly, the ablation approach differentiates the treatment planning and delivery process and also affects other factors of the workflow, such as the treatment time. In this regard, each system has accompanying software platforms designed for its specific functionalities.[7-9] However, in a general overview, the basic steps employed in the treatment workflow of external MRgFUS body systems are similar.

Before the actual treatment session, the patient's medical history should be assessed and preliminary computed tomography (CT)/MRI scans may be acquired to determine the suitability and therapeutic strategy to be followed, as well as to outline a draft treatment plan.[5] On the day of treatment, the first step in the MRgFUS workflow is patient preparation, with skin preparation (e.g., complete removal of hair and air bubbles intervening in the beam path) being crucial for achieving efficient ultrasonic transmission and avoiding skin burns.

The second step in the process is treatment planning, which involves acquiring pretherapy planning images to determine the targeted tissue and optimal treatment parameters.[5,10,11] At this step, prior planning data may be incorporated into pretherapy images. The treatment protocol is adjusted as required to minimize the risk of adverse events and ensure the best possible outcome for patients. Following segmentation of the regions of interest (ROIs), treatment volumes are distributed throughout the delineated area for ablation accounting for any sensitive structures that may interfere with the ultrasound beam and cause adverse effects.[5,10,11] The physician typically uses advanced treatment planning software to map out the treatment path by overlaying a three-dimensional (3D) map of the treatment area on anatomical images.

Before treatment delivery, the transducer is aligned with the target and low-power (nonablative) sonications are performed for focal spot verification.[6] The treatment is normally performed under conscious sedation or general anesthesia, depending on the patient's condition and preferences,[6] with the patient lying on the MRI table, typically in the prone position. Continuous monitoring, including monitoring of the patient's vital signs and MR thermometry monitoring of the temperature evolution, is required to guarantee effectiveness and safety,[5,6] also by enabling interim modifications of the plan. Thermal dose calculation may be employed complementary to temperature measurements to determine coagulative necrosis of the targeted tissue and ensure that the surrounding healthy tissue is spared. Following treatment delivery, MRI is employed for assessing the treatment outcomes. Contrast agents are typically administered to identify the coagulated region, which is characterized as the nonperfused volume (NPV).[5,6,12]

Anneveldt *et al*.[13] conducted a retrospective analysis and discussed the strategies, challenges, and outcomes encountered during the implementation of MRgFUS as a noninvasive treatment option for uterine fibroids. The study covers practical aspects of this indication, from the patient selection step to the posttreatment follow-up. Clinical outcomes, such as reduction in fibroid volume and relief of symptoms in the treated patients, are also examined. The study further underlines that the success of the procedure highly relies on a productive collaboration between medical specialists. In this context, Payne *et al*.[6] have recently published an informative guide for medical physicists regarding proper utilization of MRgFUS body systems based on the specifications of the Exablate system. Their study covers important technical considerations, safety measures, and quality assurance protocols aiming to ensure successful and effective implementation of this technology in clinical practice.

Meng *et al*.[10] outline the technical considerations of transcranial MRgFUS while presenting a range of neurological disorders where MRgFUS has shown promising results. A comprehensive overview of the technical principles and clinical workflow of transcranial MRgFUS is provided. Authors not only outline the different stages involved in the process but also discuss specific patient selection criteria and common ultrasonic and MRI monitoring protocols employed in the treatment depending on the specific neurological indication. Follow-up MRI techniques for assessing tissue response and safety measures, such as cooling techniques to prevent off-target heating, are also discussed. The importance of having a multidisciplinary team approach involving radiologists, neurologists, and neurosurgeons to ensure safe and effective implementation of the procedure is emphasized as well.[10]

There have been proposed numerous algorithms aiming to advance and optimize different aspects of the MRgFUS treatment workflow, ultimately improving the safety, efficacy, and outcome of the procedure. For instance, there are algorithms dedicated to precise segmentation and sonication path planning for full coverage of the ROIs.[11,14] In this context, the impact of different ROI coverage algorithms on critical factors of the MRgFUS workflow, such as time management and near-field heating, has been examined.[15,16] Other proposed algorithms aim to address the challenge of treating moving abdominal organs.[17,18] Indicatively, Schwenke *et al*.[18] have proposed a software tool that combines patient-specific simulation models of respiratory motion and motion tracking techniques to predict and compensate for organ motion intraprocedurally. Another noteworthy study by Zhang *et al*.[19] concerns the development of a flexible software architecture that can be used across different MRgFUS and MRI systems to guide the operator through the entire process, from the planning of treatment volumes to MRI-guided therapy under regular motion monitoring, and posttreatment assessment of NPVs. Interestingly, treatment execution is a three-phase

process involving the delivery of low and medium energy to, respectively, calibrate the beam position and dose, followed by sequential sonications using ablative energy levels.[19]

Although numerous studies offer insights into the MRgFUS workflow for treating specific indications by sharing clinical experiences, only a few have comprehensively outlined every step in the process to address practical considerations and provide specific guidelines on the proper clinical utilization of MRgFUS body systems by end users; albeit only based on the specific features of well-established commercial systems. Therefore, researchers in the preclinical field need more dedicated studies to openly exchange insights and experiences in a combined effort to address current limitations and challenges in implementing robotic-assisted FUS procedures under MRI guidance safely and effectively. This, in turn, can accelerate the adoption of this emerging technology in the treatment of a wider range of medical conditions and the clinical translation of newly developed systems and applications. The development of advanced MRgFUS software tools undeniably constitutes an integral part of this process.

The current study aimed to contribute to this effort by establishing a detailed workflow for preclinical MRgFUS studies through a series of ablation experiments in excised porcine tissue using a customized MRgFUS robotic device and accompanying software. The employed system[20] comprises a single-element spherically focused transducer of 2.6 MHz that can be moved along four PC-controlled axes (X, Y, Z, Θ). The study provides a comprehensive description of essential software functionalities and its integration with a 3T Siemens MRI scanner through the Access-I software, which allows for remote control of the scanner and direct storage and processing of MR images. Overall, an overview of the principles and workflow of a robotic MRgFUS body system is provided to the reader, which may serve as a baseline for other researchers in the preclinical field.

Materials and Methods

The present study was carried out in excised porcine tissue. No human or animal participants were involved. Therefore, no informed consent or ethical approval was necessary.

Key features of the magnetic resonance-guided focused ultrasound system

The device employed in the study consists of a mechanism enclosure hosting all the mechatronic components and a water enclosure, wherein a single-element spherically – focused ultrasonic transducer is actuated.[20] The positioning mechanism was designed with three linear and one angular piezoelectrically actuated degrees of freedom for steering the FUS beam into the subject. The water container includes a rectangular acoustic opening above the transducer's working space that is sealed with a coupling membrane, upon which the tissue of interest is placed. Degassed water is used as the coupling medium.

The system was designed to meet the specific requirements and challenges associated with robotic operation in an MRI setting. The robotic device was manufactured with MR-compatible materials having dimensions compatible with the bore size of conventional MRI scanners. A custom-made electronic driving system is externally wired to the device enabling the initiation and control of robotic movements through electronic signals. During motion, optical encoders (US Digital Corporation, Vancouver, WA 98684, USA) provide motion feedback to ensure accurate positioning of the ultrasonic source relevant to the target. The FUS system is supplied by an RF amplifier (AG1016, AG Series Amplifier, T and C Power Conversion, Inc., Rochester, USA) that is also located in the operator's room. Electronic signals are transferred by shielded cables passing through a penetration hole with integrated waveguides on the wall that separates the two rooms. Furthermore, the signals undergo filtering to ensure that interference frequencies are not transmitted into the MRI suite. The system further includes a water circulation system with integrated vacuum degassing pumps (DP-521, Baoding Shenchen Precision pump Co., Ltd, Baoding, China) and an MR-compatible camera (12M, MRC Systems GmbH, Heidelberg, Germany) for the direct visualization of acute tissue effects. Remote control of both the MRI and MRgFUS systems is available through advanced dedicated software with treatment planning and monitoring features. The diagram of Figure 1 illustrates the communication between the MRgFUS and MRI systems.

The robotic system has undergone extensive evaluation in prior preclinical studies utilizing tissue-mimicking phantoms and animal tissue and has been validated for the accuracy and repeatability of motion, MRI compatibility, and beam targeting accuracy.[21-23]

Magnetic resonance-guided focused ultrasound software

Main functionalities

The software's main programming language is C# (Microsoft Corporation, Washington, USA), whereas Python scripts (Python Software Foundation, Delaware, USA) were also incorporated to enhance its capabilities in parallel processing. It was built on the Windows Presentation Foundation platform, which allowed creating an advanced user-friendly graphical user interface (GUI), offering swift execution of commands and adaptability for future additions.

The software acts as the central control hub, facilitating communication, and synchronization among the different system components. Figure 2a shows a schematic diagram of the software connection with the various peripheral devices. Figure 2b is a screenshot of the main software window that includes the treatment planning window and main toolbar (left side) with the various other functionality GUI buttons available. The software interfaces with the MRI system through Access-I for directly transferring imaging data and retrieving Digital Imaging and Communications in Medicine (DICOM) images from the scanner for both treatment planning and monitoring purposes.

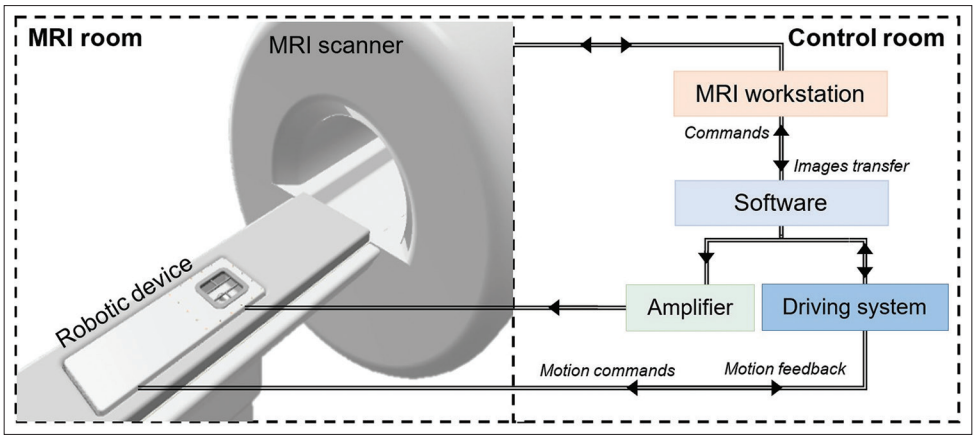

Figure 1: Wiring diagram indicating the connection among components of the magnetic resonance imaging and magnetic resonance-guided focused ultrasound systems. MRI: Magnetic resonance imaging

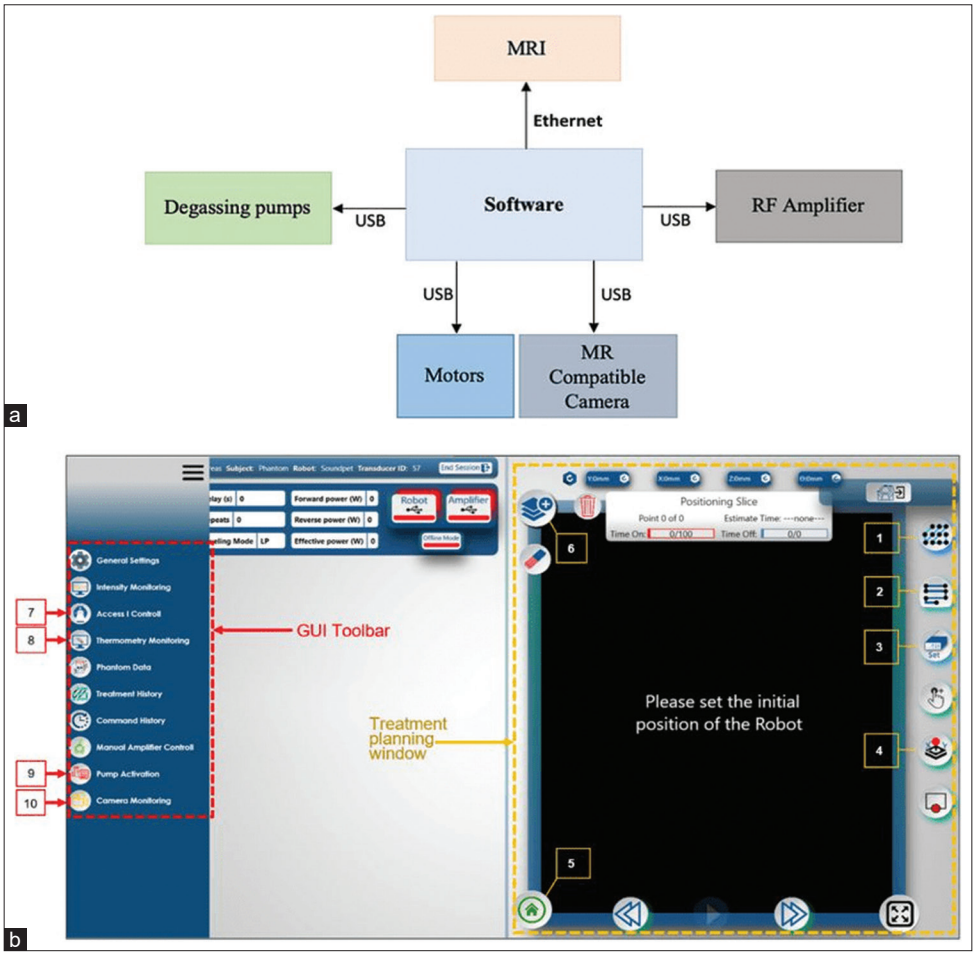

Figure 2: (a) Schematic diagram of software connection and communication with peripheral devices. (b) Screenshot of the initial main software window with the treatment planning window and the various functionality graphical user interface buttons: (1) Drawing tool panel, (2) Sorting type menu, (3) Amplifier setup menu, (4) Manual motion control, (5) "Homing" process, (6) Layer creation, (7) Access-I control, (8) Thermometry monitoring, (9) Pump activation, and (10) camera monitoring. MRI: Magnetic resonance imaging, MR: Magnetic resonance

Treatment planning is performed on preoperative DICOM images, where the ablation pattern is determined by the user using one of the three manual design options available in the drawing tool panel: (1) distribution of random sonication points, (2) selection of a rectangular area and specific motion resolution (grid sonication pattern), or (3) semiautomatic selection of a nonuniform area (irregular sonication pattern). In the latter case, the sonication pathway for full coverage of

the segmented region is automatically generated by a dedicated algorithm utilizing a zigzag pattern.[14] Otherwise, the user can select the desired sorting type among sequential, spiral, or zigzag, determining the order in which the various sonication points will be visited (sorting type menu). The extracted motion commands are then sent by the software to the motors through a Universal Serial Bus (USB) port to dynamically adjust the ultrasonic beam according to the planned sonication protocol. There is also a GUI panel dedicated to controlling the power output of the amplifier (amplifier setup menu), which also connects with the software through USB interfaces.

Moreover, communication with an external water degassing system was successfully attained, enabling control of water inlet and circulation within the water container of the robotic device to ensure degassing of the water surrounding the transducer. In addition, the same system ensures transducer cooling and cooling of the skin surface in future clinical use (pump activation). Real-time visual inspection of the in-bore procedure is available on the software utilizing the MRI-compatible camera (camera monitoring).

Access-I

A major functionality added to the software is the Access-I that enables remote control of MAGNETOM MRI scanners manufactured by Siemens Healthineers (Erlangen, Germany). Specifically, the MRgFUS software was interfaced with a 3T Magnetom Vida scanner to establish a complete and efficient workflow. The Access-I software package was initially installed on the relevant scanner, acting as a middleware layer facilitating the communication between the scanner and the MRgFUS software. The existing software was then adapted by incorporating two Access-I functionalities utilizing dedicated software development kits provided by Siemens and according to the specific guidelines provided in the Access-I Developer Guide document.

The first functionality establishes a passive connection with the Access-I server of the scanner based on a Python script that allows for real-time image storage and processing. The second functionality establishes an interactive connection with the scanner enabling remote overall control and triggering of the MRI system. This interactive functionality can be simply activated by double-clicking on the "Access-I" button on the toolbar of the main window [Figure 2]. The relevant panel includes the three main subpanels as shown in Figure 3. The user should initially request access to the Access-I functionality and then control the MRI scanner. Note that planning of imaging sequences was not employed under this functionality. The sequences are planned as normally on the MRI console and collected in a list at the "available programs" subpanel, provided that they were previously made available to the software by attaching the Access-I Dot-AddIn within the Dot Cockpit interface of the scanner. The sequences of interest are then moved by the user to the "templates in the queue" subpanel. The ones to be executed are finally transferred to the "executed templates" subpanel, from which they can be manually started. Furthermore, the user can select from this list the desired sequence to be used for thermometry by clicking the "use for thermometry" button [Figure 3] and then initiate online thermometry through the relevant thermometry monitoring panel of the main window toolbar [Figure 2].

As a result, the software allows interactive remote control of the MRI scanner and access to imaging data. The scanner can be remotely triggered to initiate imaging, whereas the acquired images are directly transferred to and processed by the software in near real time for monitoring purposes. The user can terminate a sequence at any time if necessary.

Magnetic resonance thermometry and thermal dose calculation

The real-time acquisition and transfer of MR images through Access-I allowed the integration of MR thermometry tools in the software. The main treatment planning software runs in parallel to a separate MR thermometry script written in Python for dynamically generating and displaying temperature and thermal dose maps during the execution of the planned sonication protocol.

During ultrasonic heating, the software determines the temperature changes within the ROI by employing the proton resonance frequency (PRF) shift method.[24] This method involves comparing the phase between an initial baseline image acquired at a reference temperature (φ_0) and subsequent images taken at different time points intra- and postprocedurally (φ). These phase changes arise from the temperature-dependent PRF changes in the ROI and can be converted into the respective temperature changes (ΔT) by applying the following relation:

$$\Delta T = \frac{\varphi - \varphi_0}{\gamma \alpha B_0 TE} \quad [1]$$

where γ is the gyromagnetic ratio, α is the PRF change coefficient, B_0 is the magnetic field strength (3T), and TE is the echo time. The maps are typically constructed using a two-dimensional (2D) fast low-angle shot (FLASH) sequence.

The thermal dose is used as the main metric for assessing whether tissue necrosis has been successfully achieved. The software calculates the thermal dose according to the method proposed by Sapareto and Dewey using the following equation:[25]

$$CEM\,43°C = \sum_{t=0}^{t=final} R^{(43-T)} \Delta t \quad [2]$$

where $CEM43°C$ is the cumulative number of equivalent minutes at 43°C, T is the average temperature during the elapsed time Δt, and R is the temperature-dependent rate of cell death (a constant of 0.25 is used for temperatures smaller than 43°C and 0.5 for temperatures higher than 43°C). In general, a thermal dose equal to 240 $CEM43°C$ is considered sufficient for achieving coagulative necrosis of tissue (i.e., the tissue needs to be exposed to a cumulative equivalent of 240 min at 43°C).[26,27]

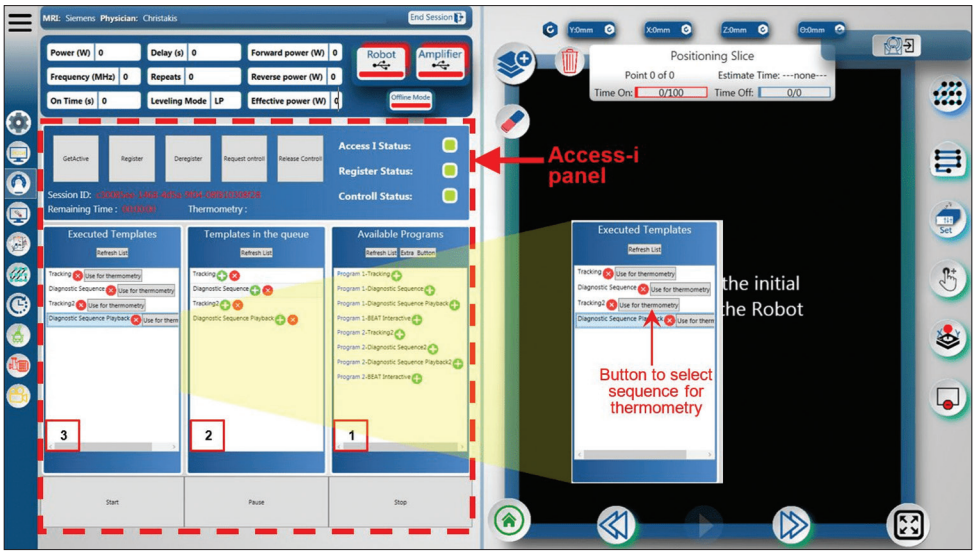

Figure 3: Screenshot of the Access-I panel with three main subpanels: (1) Available programs, (2) Templates in the queue, and (3) Executed templates

The treatment monitoring tools are available in the thermometry monitoring panel [Figure 2], which is divided into several subpanels enabling the user to set essential parameters required for MR thermometry (e.g., number of reference images, T tolerance, and thermal dose threshold) and visualize dynamic temperature maps, thermal dose maps, necrosis maps, and time-series temperature data in parallel. The estimated temperatures and accumulated thermal dose are represented as color-coded maps, which can be overlaid on anatomical images to provide a comprehensive visualization of the treatment area. Notably, the thermal dose values are expressed in a color-coded (blue-to-red) logarithmic scale. The simulated area of tissue necrosis is also overlaid on the corresponding magnitude image of the subject as a red region. Quantitative information on the necrotic region (i.e., the extent of necrosis in mm^2) is also extracted automatically and displayed on the relevant monitoring panel and updated for each individual sonication and timepoint during treatment. In addition, the software identifies and indicates to the user the regions that did not receive ablative thermal dose during the initial sonication and should be re-exposed. This process may require adjusting the FUS parameters (e.g., the acoustic intensity and duration) to deliver sufficient thermal dose for tissue necrosis in the relevant regions.

Treatment workflow

The main steps followed for performing an MRgFUS procedure with the proposed preclinical robotic system are summarized in the workflow diagram of Figure 4. The first step in the MRgFUS workflow concerns the positioning and registration of the robot in the MRI coordinates. Localizer images are initially acquired to assess successful subject-transducer setup and determine the appropriate FOV for subsequent sequences. For instance, air bubbles may be identified in the treatment pathway and removed using the degassing pumps, thus optimizing the acoustic coupling. Transducer tracking in the MRI coordinates and identification of the ROI in relation to

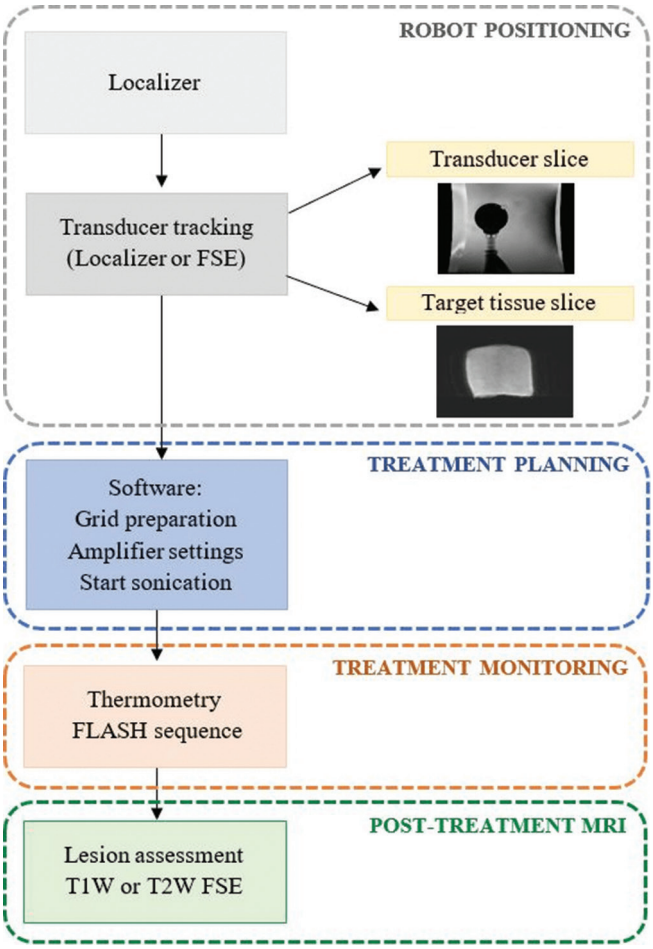

Figure 4: Schematic diagram of the treatment workflow with the proposed magnetic resonance-guided focused ultrasound software. FSE: Fast spin echo, FLASH: Fast low angle shot

the transducer home position is simply achieved by acquiring parallel slices at the level of the transducer (located at the axes origin) and targeted tissue. Fast spin echo (FSE) sequences

are typically employed for this purpose, or the localizer images may be used alternatively. Once the user specifies the transducer location, a marker appears at its center, which is subsequently superimposed onto the DICOM images utilized for treatment planning.

The treatment planning process begins with the creation of a layer on a specific DICOM image of the subject, which includes an overlay of the transducer position and available working area, as defined by the motion range limits of the robot. The user specifies the Z-position of this specific layer, which is then translated into the corresponding height along the Z-axis of the device so that ultrasonic energy can be delivered to the particular layer.

The next planning step involves defining the region for ablation and motion parameters (step size and sorting type), followed by the automatic prescription of sonication foci to cover the ROI. The amplifier parameters (power, frequency, and sonication duration) and time delay between successive sonications are then defined by the user. Notably, for treatment in a 3D space, the planning procedure should be repeated for multiple layers at different heights (Z-axis).

Before initiating sonication, the user should select the desired sequence for thermometry from the Access-I panel and initiate the process through the MR thermometry monitoring panel. After the acquisition of at least three reference images, the sonication protocol can be activated. A test low-power sonication may be carried out once the transducer is moved to the first point of sonication to verify the accurate location of the focal point before proceeding to full-power sonication.

During execution of the planned sonication, a multifold monitoring approach is available combining FLASH-based temperature, thermal dose, and necrotic area mapping. The latest thermometry data are displayed on-screen at time intervals equal to the image acquisition time of the employed MR imaging sequence. The necrosis map is overlaid on anatomical images of the ROI revealing potential "viable" regions where sonication should be repeated. The software returns a true or false value for each sonicated point indicating the presence or absence of necrosis, respectively. Thereby, the user can repeat unsuccessful sonications following adjustment of the sonication protocol if required.

By the end of the sonication, T1-weighted (T1-W) or T2-weighted (T2-W) FSE imaging is employed for assessing the treatment effects, including lesion formation and potential off-target tissue effects.

Magnetic resonance-guided focused ultrasound ablation in *ex vivo* porcine tissue

The robotic device was placed on the table of the 3T Magnetom Vida scanner as shown in Figure 5. A piece of freshly excised porcine tissue was securely positioned on the acoustic opening. Degassed water was used to completely fill the space between the membrane and tissue to allow for efficient ultrasound transmission. A plastic structure was attached on the MRI

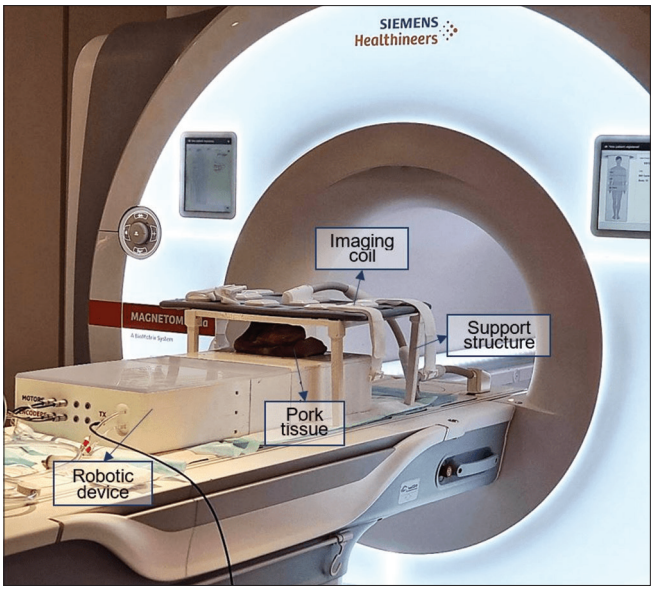

Figure 5: The experimental setup for magnetic resonance-guided focused ultrasound ablation of *ex vivo* porcine tissue in the 3T Siemens magnetic resonance imaging scanner

table to support the imaging coil at a small distance above the ROI. Notably, isolation of the coil from the sonicated sample is considered essential to prevent the transfer of vibrations to the coil.[21]

A single-element spherical focused transducer (Piezohannas, Wuhan, China) with a frequency of 2.6 MHz, diameter of 50 mm, radius of curvature of 65 mm, and efficiency of 30% was employed in all the experiments. The tissue sample was sonicated in different grid patterns with varying spatial steps and a 60-s delay between sequential sonications. Each grid spot was exposed at an acoustic power of 75–90 W for 20–30 s, with the focal depth set at 35 mm. The tissue effects were monitored using MR thermometry according to equation[1], where the magnitude of α was set at 0.0094 ppm/°C.[28] The temperature and thermal dose distribution were mapped on a pixel-by-pixel basis by the dynamic acquisition of 2D FLASH images with repetition time (TR) =25 ms, echo time (TE) =10 ms, flip angle (FA) =30°, echo train length (ETL) =1, pixel bandwidth = 250 Hz/pixel, field of view (FOV) =280 mm × 280 mm × 3 mm, acquisition matrix size = 96 × 96, and acquisition time/slice = 2.4 s, using the multichannel Spine 72 RS coil (Siemens). It is important to note that before executing each planned sonication protocol, a preliminary low-power sonication was performed to confirm precise beam focusing at the desired tissue depth, as well as proper communication between the MRI and robotic systems and the functioning of all monitoring tools.

Postsonication assessment of lesion formation included T2-W imaging followed by tissue dissection to determine the actual size of lesions. T2-W FSE images were acquired with a multichannel body coil (Body18, Siemens) using TR = 4000 ms, TE = 52 ms, FA = 110°, ETL = 20, pixel bandwidth = 250 Hz/pixel, FOV = 245 mm × 261 mm × 3 mm, matrix size = 256 × 240, and slice thickness = 3 mm.

The efficacy and reliability of the proposed MRI-based monitoring tools were examined by cross-referencing the data extracted by the software with the observed tissue damage in postdissection analysis. Similar approaches are adopted in both preclinical and clinical settings to assess the effectiveness of MRI-based monitoring methods of FUS-induced tissue effects by comparing the MRI output with the actual degree of tissue damage as observed postsonication by histological examination.[29-31]

Results

MRgFUS ablation of *ex vivo* porcine tissue was successfully performed without any identified FUS-related off-target effects, thus demonstrating an efficient procedural workflow. Indicative results of the MRgFUS procedure from treatment planning to postsonication assessment are presented in Figures 6–11.

The first example concerns a 6 × 6 rhomboid grid, where each spot was exposed at 75 W acoustic power for 30 s, using a 60-s delay between adjacent sonications. The spatial step was set at 10 mm in both the X- and Y-axes. Figure 6 is a screenshot of the software acquired during the execution of the planned sonication. As shown, the software interface allowed the user to visualize in real time the temperature, thermal dose, and necrosis evolution in the relevant monitoring subpanels. Note that the treatment planning window appears at the right side of this window showing the planned sonication pattern overlaid on the relevant reference image of the tissue.

Figure 7 is a collection of thermal maps acquired during the 6 × 6 sonication, providing a visual representation of the temperature distribution within the imaged region over time, with the color scale ranging from yellow to red representing temperatures from the lowest to the highest value. The temperature profiles recorded at the various focal spots during the sequential sonications are combined in the graph of Figure 8, where the various peaks indicate the maximum temperature achieved in each sonication spot. The maximum recorded temperatures (i.e., at the focal point) varied from a minimum value of 67°C to a maximum value of 93°C. This graph illustrates the development of ablative temperatures at each of the 36 sonicated points. This graph further reveals a clear increase in the baseline temperature with time owing to heat dissipation from previously sonicated areas.

Figure 9 provides a visual representation of the accuracy and effectiveness of the sonication. The planned sonication foci can be seen in the software screenshot of Figure 9a. Tissue necrosis was successfully monitored interprocedurally by dynamic thermal dose and necrotic area mapping, resulting in the final maps of Figures 9b and c, respectively, following the completion of the sonication. The tissue effects were directly examined by T2-W FSE imaging and then by visual examination. An indicative MR image and a photo of the sonicated tissue are, respectively, shown in Figure 9d and e. Note that the mean lesion diameter as measured on the T2-W image of 6.6 ± 0.8 mm was smaller than the actual lesion size of 7.6 ± 0.9 mm measured with a caliper (0.1 mm resolution). Note also that the thermal dose and necrosis maps, as well as the actual coagulative lesions revealed on tissue dissection, were in excellent agreement with the planned sonication pattern. All inflicted lesions were located at the desired tissue depth of 3.5 cm corresponding to the transducer's focal depth (as defined during the planning process). The average lesion diameter extracted from the software based on the simulated thermal dose is 7.59 ± 0.57 mm, almost matching the mean value estimated by digital caliper measurements [Figure 9e].

The overlapping lesion shown in Figure 10 was created by sonication in an irregular pattern [Figure 10a] using similar acoustic power applied for 20 s, a smaller cooling time of 60 s, and a smaller spatial step of 3 mm. The T2-W image of the sonicated tissue revealed an oval lesion area of 13.6 cm^2 [Figure 10b] compared to the actual area of 17.5 cm^2

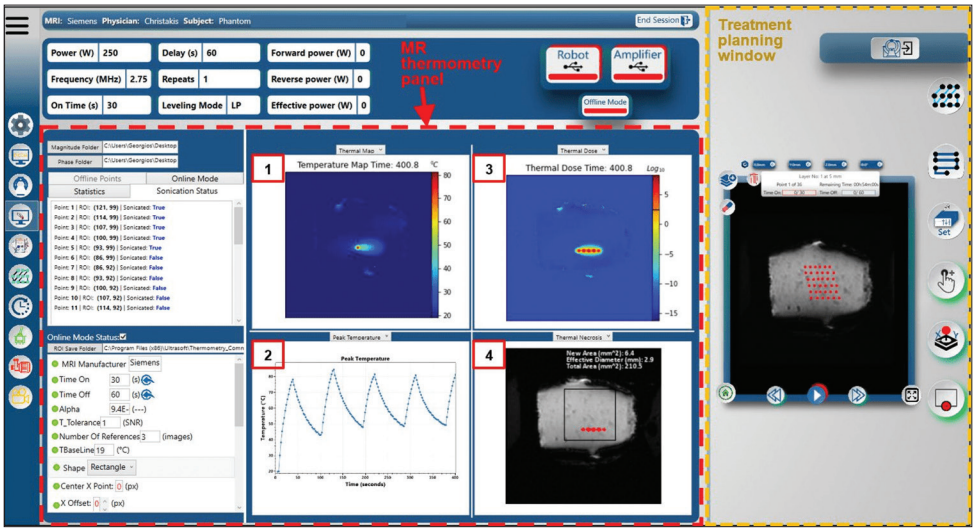

Figure 6: Screenshot of the software with the magnetic resonance thermometry monitoring panel activated, indicating the 4 main subpanels: (1) thermal maps, (2) thermal dose maps, (3) a time-series temperature graph, and (4) thermal necrosis area overlaid on magnitude image

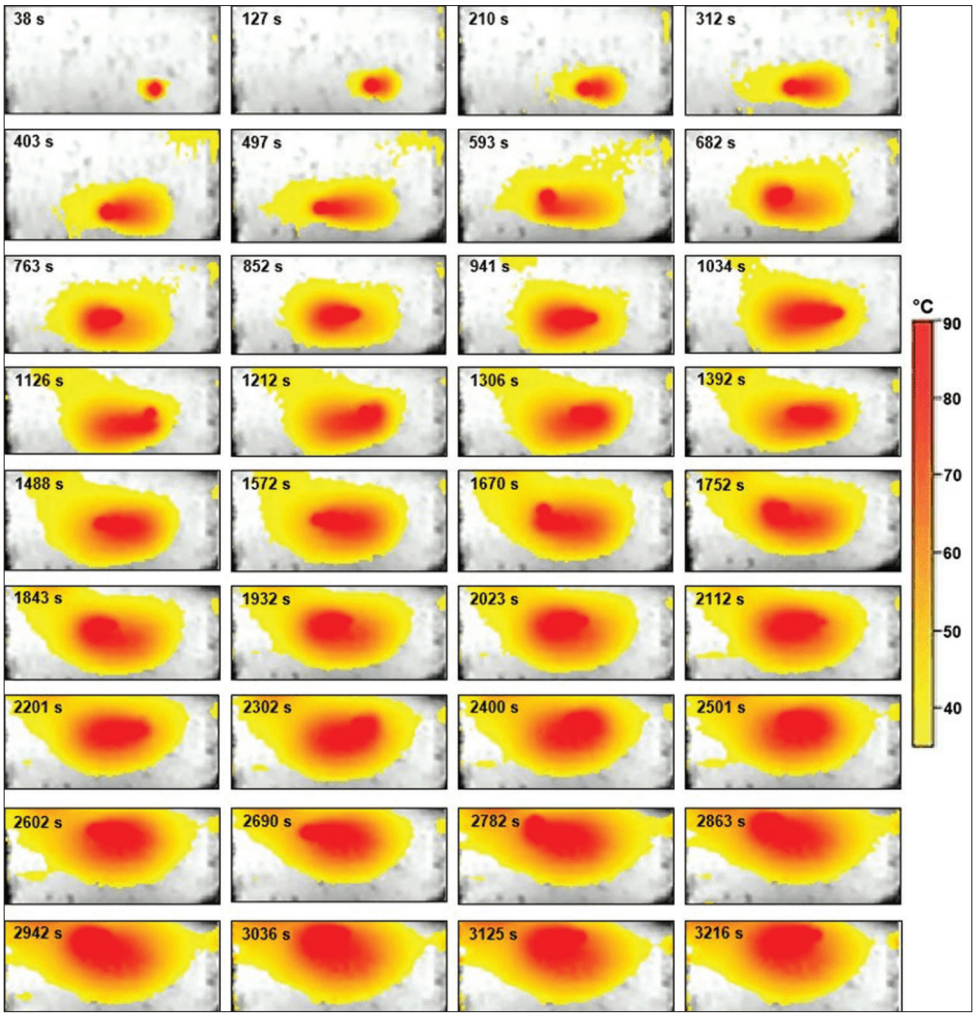

Figure 7: Coronal thermal maps acquired at the focal spot level using fast low-angle shot sequence showing the temperature evolution during the 6 × 6 sonication

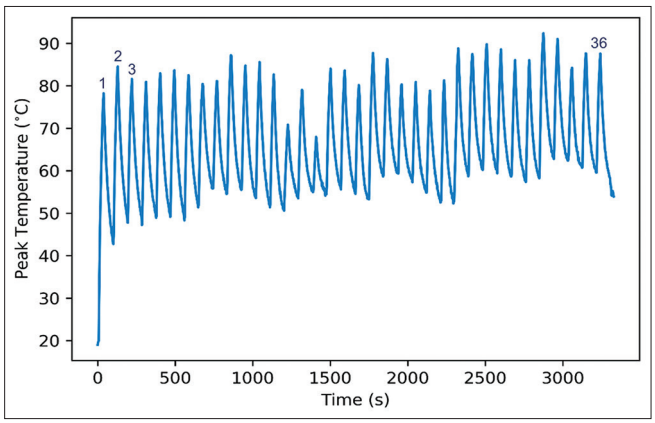

Figure 8: Time series plot of the focal temperature evolution during the 30-s of sonication and 60-s time delay at each of the 36 sonicated points

measured on the tissue slice [Figure 10c]. On the contrary, a good match was found between the simulated lesion size, as determined by thermal dose accumulation, and the measured lesion size (~17 cm^2).

Finally, Figure 11 presents the results of a test conducted to evaluate the software's capability to accurately identify regions where incomplete necrosis occurred. For this purpose, the amplifier was intentionally deactivated at two random points (No. 6 and No. 10) of a 4 × 4 grid pattern, simulating a particular scenario where sonication at these specific points was unsuccessful, potentially due to obstacles obstructing the beam pathway or an amplifier malfunctioning. In that case, each spot was exposed at 90 W acoustic power for 30 s using a step of 15 mm and leaving a 60-s delay between them. As shown in Figure 11a, the accumulated thermal dose remained below the set threshold for necrosis (240 *CEM*43°C), indicating that tissue necrosis was not achieved in these specific regions. The software successfully generated the corresponding necrosis map as shown in Figure 11b, which coincides perfectly with the thermal dose map, indicating the regions of tissue that are spared and should be re-sonicated. Figure 11c shows the list of the sonication status returned to the user. Note that the relevant points (No. 6 and No. 10) have a "false" status, whereas the remaining points are flagged as "true," proving the software's

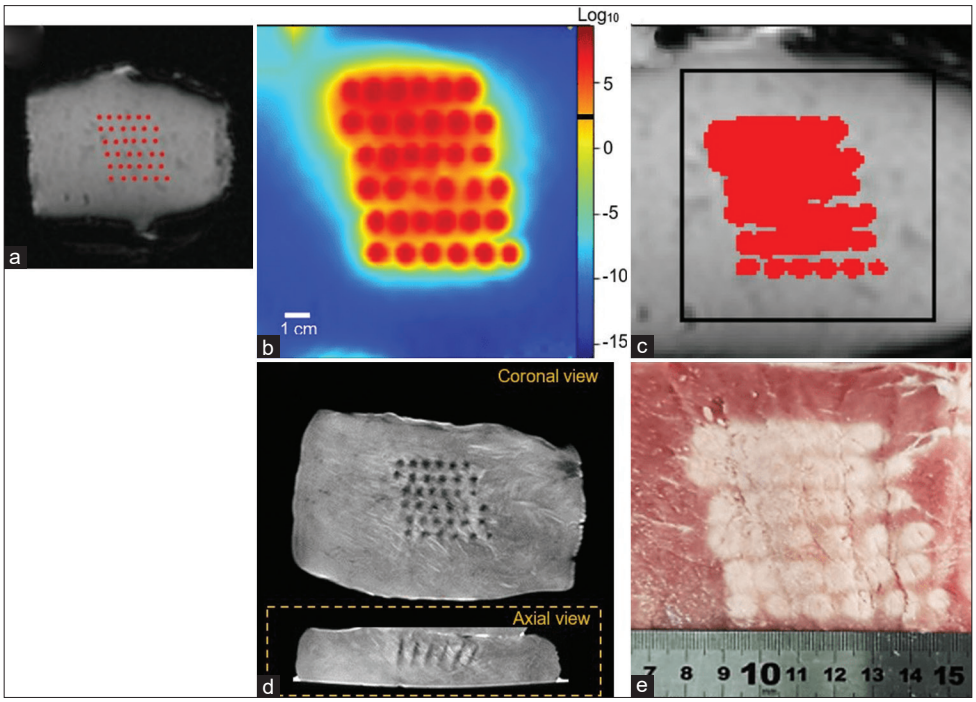

Figure 9: (a) The 6 × 6 sonication pattern as planned on the Digital Imaging and Communications in Medicine image of the sample tissue. (b) Thermal dose map after the end of sonication expressed in log scale. The black bar corresponds to a thermal dose of 240 CEM43°C. (c) The necrosis map after the end of sonication. (d) Postsonication T2-weighted Fast Spin Echo coronal image of tissue showing the 36 formed lesions and axial image showing the lesions formed in a random grid row. (e) Photo of the tissue following dissection revealing the actual formed lesions

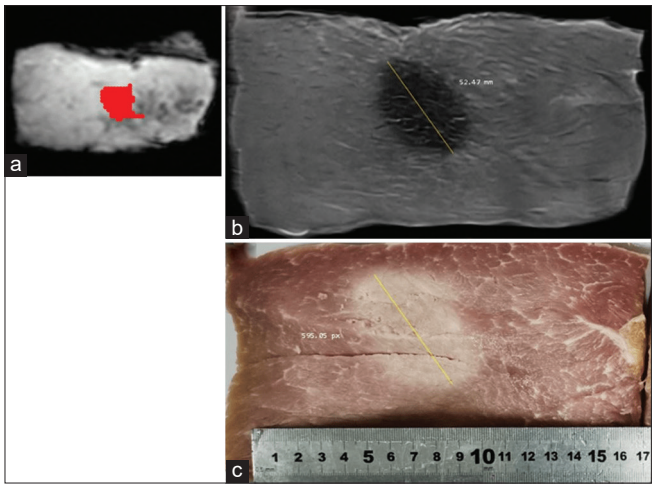

Figure 10: (a) Irregular sonication pattern (overlapping) as planned on the Digital Imaging and Communications in Medicine reference image of the porcine tissue sample. (b) Postsonication T2-weighted Fast Spin Echo coronal image of the tissue. (c) Photo of the tissue following dissection revealing the actual formed lesion

ability to accurately identify and indicate to the user which specific grid points should be revisited.

Discussion

The current study outlines the various steps involved in the MRgFUS workflow utilizing a preclinical MRgFUS body system and accompanied software. A thorough description of essential software features and how these were enhanced by incorporating Access-I functionalities to allow remote triggering of Siemens Magnetom scanners and real-time access to imaging data is provided. The effectiveness of the employed MRgFUS system is demonstrated by providing indicative results of MRgFUS ablations in *ex vivo* animal tissue. In this context, an efficient procedural workflow, from treatment planning to intraprocedural MR thermometry-based monitoring and postsonication MRI assessment of acute tissue effects, is established. Remarkably, the creation of a comprehensive MRgFUS preclinical workflow could serve as the basis for the protocol optimization of MRI-compatible FUS robots.[20,32,33]

In commercially available MRgFUS body systems, electronic steering is used to scan the beam throughout the target volume and is sometimes performed complementary to the mechanical positioning of the source depending on the ROI size.[3,4] The application of single-element ultrasonic sources has been so far limited to commercial systems for US-guided interventions,[34,35] also extending to preclinical MRgFUS research. In fact, a wide spectrum of preclinical MRI-compatible FUS systems employing single-element transducers exist in the scientific literature.[20,36-40] In both preclinical and clinical settings, mechanical scanning of single-element FUS sources is a common practice to ablate adjacent locations within the target. Consequently, outlining the steps of an effective procedural workflow in preclinical MRgFUS studies could streamline the evaluation process of newly developed systems and emerging applications, potentially facilitating their translation into clinical practice and the beginning of new eras in clinical MRgFUS practice.

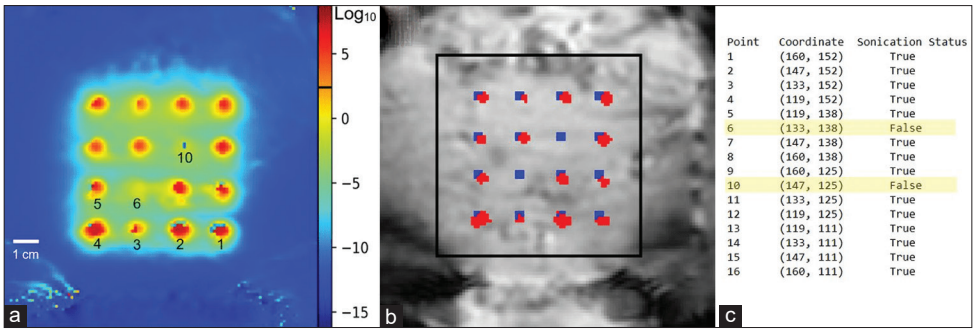

Figure 11: Example of unsuccessful sonication: (a) The thermal dose map after a 4 × 4 grid sonication where the amplifier was deactivated at points No. 6 and No. 10. The black bar corresponds to a thermal dose of 240 CEM43°C. (b) The corresponding necrosis map; the necrotic regions appear in red and planned sonication points in blue. (c) The sonication status list returned to the user indicating the two points that were not successfully sonicated

The main innovation of the MRgFUS system employed in this study lies in its unique design featuring a single-element transducer and a simplified robotic mechanism, which not only enhances cost-effectiveness but also ensures operational simplicity. The system's universal and compact design is expected to allow its seamless integration into any conventional MRI scanner. In commercial MRgFUS systems, the need to control each array element individually results in the need for advanced signal processing algorithms,[41] unavoidably complicating and prolonging the procedure. Contrarily, the proposed system simplifies the overall treatment workflow remarkably. Simplifying the workflow of an MRgFUS procedure can offer multiple benefits. First, it can lead to increased efficiency while also reducing the overall time required for the procedure. This not only benefits the patient by minimizing their time spent in the scanner but also optimizes resource utilization in the MRI setting, potentially lowering the treatment costs. A streamlined process can also enhance safety by minimizing the potential for errors and complications. In addition, a simplified medical device with a well-established operation workflow will require less specialized training, thereby being accessible to a broader range of medical professionals. It may also facilitate the wider adoption of the technology by medical facilities since it will be easier to be integrated into their existing clinical workflow.

Various MRgFUS protocols were planned and executed by the employed MRgFUS system with high precision and accuracy. Successful communication between the MRgFUS and MRI systems was established through dedicated Access-I functionalities, enabling the software to directly retrieve DICOM images of the porcine tissue sample and remotely trigger the MRI for the acquisition and display of MR images in actual time. MR thermometry monitoring of tissue ablation was successfully performed with a quite fast pulse sequence. The monitoring panel allowed the user to monitor the FUS-induced tissue effects through a dynamic display of temperature maps, thermal dose maps, and the simulated necrotic region overlaid on magnitude images of the subject [Figure 6]. The software was also proven efficient in determining whether tissue necrosis was successfully achieved and indicating to the user the specific grid points that should be re-sonicated [Figure 11].

The positioning mechanism precisely navigated the ultrasonic beam aligning it with the desired treatment locations within the porcine tissue sample. The selected ultrasonic parameters resulted in tissue necrosis (accumulated thermal dose >240 *CEM*43°C), also confirming that an efficient coupling with the target was achieved. In general, it was previously demonstrated that maintaining tissue temperature above 55°C for 1 s or longer causes instantaneous tissue death by thermal coagulation.[42] In the case of the 6 × 6 grid where the various sonication points were exposed at a focal intensity of about 17440 W/cm^2 for 30 s, the recorded focal temperatures reached 67–93°C, depending on the specific tissue characteristics (e.g., the presence of fat and inhomogeneities) and prefocal heat accumulation. The thermal dose distribution and simulated necrotic regions were highly consistent with the intended sonication pattern [Figure 9].

Postsonication T2-W images showed a decrease in the signal intensity of the treated points, which served as an additional indication of successful sonication. The pattern of inflicted lesions as visualized on the T2-W images agreed well with the planned sonication pattern, thermal dose distribution, and simulated regions of necrosis [Figure 9]. Being in agreement with prior literature, the present findings reveal that MRI imaging may underestimate the size of FUS lesions,[43] potentially owning to limitations in spatial resolution or inability to precisely delineate the lesion borders. Consequently, it is crucial for researchers to consider increasing the imaging resolution or possibly using other pulse sequences to ensure an accurate assessment of the extent of tissue necrosis following MRgFUS procedures. Notably, T1-W imaging may be preferable for lesion assessment in live tissue owing to the utilization of contrast agents. In general, high-resolution FSE imaging of the formed lesions is not considered the method of choice for determining the lesion size, but it can though provide valuable information on successful ablation and lesion formation.

Finally, a visual examination of the sonicated tissue confirmed that the formed lesions were precisely inflicted in tissue in the desired arrangement [Figure 9]. The agreement between planned and delivered sonications, as well as between

MR-based thermal dose mapping and postsonication caliper measurements in terms of the lesions' depth, size, and spacing, constitutes sufficient evidence of the accuracy of ultrasonic delivery, reliability of the treatment monitoring algorithms, and robust interoperability between hardware and software. Note that the slight deviation in diameter among lesions is reasonable and anticipated due to the inhomogeneities of porcine tissue. Remarkably, none of the assessment methods revealed FUS-related off-target effects.

In this study, a cooling time of 60 s between consecutive sonications was considered sufficient to mitigate prefocal heating phenomena.[16] However, the time-series plot of recorded temperatures [Figure 8] reveals clear evidence of heat dissipation among neighboring grid points (6 × 6 grid). Note that following the completion of each sonication, the subsequent sonication point could not return to the baseline temperature within the 60-s cooling time, thus resulting in a progression increase in the baseline temperature over time. This unavoidably led to an increasing heat accumulation [Figure 9b] and extends of tissue necrosis as the sonication pattern progressed toward its final points. Consequently, the discrete lesions gradually increased in diameter, ultimately merging into overlapping lesions within the final two (top) rows of the sonication grid [Figure 9e]. It is thus crucial that during the planning process, the prefocal thermal dose accumulation is accounted to avoid damage to healthy tissue. In this context, cooling of the skin surface is also required to avoid skin burns, which constitute the most common FUS-induced complications, with the typically reported rates being up to 10%.[44,45]

Successful implementation of the planned sonication protocols further demonstrates the system's compatibility with the MRI. In this context, optimization of the coil position is deemed essential in achieving satisfactory signal-to-noise ratio values for high-quality imaging and thermometry.[21] A specific measure employed in this study is the isolation of the coil from the subject so that during sonication potential subject vibrations are not transferred to the coil. In addition, the mechatronic parts of the robot were not included within the coil imaging area to minimize the possibilities for susceptibility artifacts. In general, the operator should select the coil position carefully to ensure adequate proximity to the region of interest but not direct contact with the subject and the absence of any interference with the beam. Notably, in clinical systems employing the phased array technology, MR thermometry is typically performed during electronic beam steering and not, whereas the transducer is moving to avoid the introduction of susceptibility artifacts in thermal maps.[6]

A potential limitation of these experiments is that sonications were limited to a single layer for the sake of simplicity, and thus, only the horizontal motion stages were activated. The described planning procedure could be repeated for multiple layers to enable treatment in the 3D space. Motion along the Z-axis will be required in the case of sonicating different Z-layers. Furthermore, in the case of *in vivo* application, beam angulation will most likely be necessary to prevent beam interference with critical structures such as bones and air regions.

Although the focus of this work was to propose an efficient procedural workflow tailored to preclinical FUS systems operating within an MRI scanner, the key steps and concepts outlined herein are applicable to the clinical setting as well. In the case of clinical phased array systems, visiting successive sonication points could have been achieved by beam steering instead of transducer displacement. While in the general sense, the presented workflow applies also in the clinical scenario, there exist additional considerations regarding applications in human subjects and complementary strategies should be adopted to account for clinically relevant factors. The present study was carried out in excised porcine tissue, which is considered an adequately representative preclinical model owing to the anatomical and physiological characteristics it shares with human tissue. It thus provides a controlled environment to establish proof of concept and optimize emerging systems and applications before *in vivo* studies. Nevertheless, when it comes to clinical usefulness, this model has critical limitations, including the absence of blood flow and movement. Patient motion, far-field protection, and skin preparation are some of the safety considerations that should be taken into account within the clinical workflow.[6] In addition, continuous monitoring of patient's physiological parameters is mandatory in the clinical practice and immediate response actions should be in place to mitigate potential risks.

Regarding motion management strategies, there are already established methods, such as immobilization and gating techniques that could be used.[46] There is also the possibility to incorporate motion compensation algorithms in the software to account for involuntary patient movements during the procedure and ensure accurate targeting, especially for abdominal targets. Accordingly, the next step in advancing the presented software is to incorporate motion compensation functionality.

Another essential safety measure considered critical for *in vivo* applications but not discussed in this study is the employment of a thermal dose verification sonication within the treatment planning process.[6] Such verification sonication is conducted to assess whether the predicted power levels for achieving the desired thermal dose accumulation are either excessive or insufficient, given that the temperature elevation is influenced not only by the energy applied but also by the intricate heat transfer mechanisms within tissues. Thereby, thermal dose testing is crucial to determining if any protocol calibration is required. Furthermore, the present study does not concern pretreatment planning imaging, neither short- or long-term follow-up.[5]

The treatment duration constitutes an additional consideration not addressed herein. MRgFUS is a relatively time-consuming procedure, especially when it comes to ablating large and challenging tumors. The long duration of such procedures

may pose significant challenges in efficient MRI resource utilization since it can limit the availability of MRI machines for other diagnostic and interventional procedures. Although more crucial for clinical applications, the procedure duration is an important factor in preclinical MRgFUS studies as well. Optimization of the procedural workflow is crucial in improving the time efficiency of MRgFUS. Researchers should thus carefully plan and optimize experimental protocols to make efficient use of the limited MRI time available. As previously discussed, multiple sonications are required to cover the entire region of interest and a certain cooling time should be left between them to avoid damaging off-target regions. Optimized scanning algorithms can be employed to reduce the required cooling time and speed up the treatment process.[16] Other potential measures that could be considered include the implementation of fast motion algorithms and high-speed robotics, comprehensive planning to prevent complications and the necessity to repeat sonications during the procedure, continuous upgrade of software/hardware features and imaging systems, and the establishment of standardized protocols for commonly performed procedures.

Regarding the robotic device utilized in the present study, its translation into the clinical environment would entail relatively simple modifications, these being scaling up to expand the motion range and adjusting the transducer's frequency depending on the target's nature and depth. The latter adjustment necessitates the use of exchangeable transducers.

While commercial systems come equipped with sophisticated software, only their basic features are disclosed to the scientific community without adequate details. A more transparent and comprehensive description of dedicated treatment planning and monitoring software tools can provide a practical guidance for other researchers in the field. Advantageously, this study provides a comprehensive description of the Access-I functionalities incorporated in the software to allow remote control of the scanner and the direct storage and processing of acquired images. To the best of the authors' knowledge, there is a lack of prior documentation on this topic. The absence of relevant documentation constitutes a significant challenge for the researchers, who encounter difficulties in establishing an efficient workflow in MRgFUS studies and waste valuable time to uncover insights that could have been extracted from the existing literature. Therefore, this study holds the potential to benefit other researchers in the field and accelerate future studies by enabling a basic understanding of the Access-I functionality. However, it is important to highlight that integration of any software in the Access-I MR Scanner Interface should be performed following the specific guidelines provided in the Access-I Developer Guide of Siemens and according to the unique features and intended application of the software.

Conclusions

Overall, the study outcomes prove the effectiveness of the employed MRgFUS system in accurately planning and executing MRgFUS protocols. The employed software integrates all the key functionalities required for establishing an efficient MRgFUS workflow, including the direct acquisition of MRI images, transducer localization, treatment planning, and automatic execution of the planned sonication protocol under continuous software-based monitoring of the thermal dose accumulation and tissue necrosis in near real time. While these functionalities are satisfactory for preclinical applications, they should be potentially enhanced (e.g., to allow for motion compensation) to enable clinical translation. Through this paper, a comprehensive overview of the MRgFUS workflow of a preclinical body system is provided to the reader, highlighting critical aspects and potential matters of concern in establishing a successful workflow and maintaining optimal conditions for the delivery of MRgFUS. Therefore, it could be of benefit to researchers in the field aiming to implement similar preclinical studies, simultaneously contributing to advancing the understanding of how to develop MRgFUS applications that could be more easily translated to the clinic.

Financial support and sponsorship

The study was co-funded by the European Structural and Investment Funds (ESIF), Recovery and Resilience Plan of the European Union, and the Republic of Cyprus through the Research and Innovation Foundation (RIF) under the projects SOUNDPET (INTEGRATED/0918/0008) and FUSVET (SEED/1221/0080).

Conflicts of interest

There are no conflicts of interest.

References

1. Lee EJ, Fomenko A, Lozano AM. Magnetic resonance-guided focused ultrasound: Current status and future perspectives in thermal ablation and blood-brain barrier opening. J Korean Neurosurg Soc 2019;62:10-26.
2. Izadifar Z, Izadifar Z, Chapman D, Babyn P. An introduction to high intensity focused ultrasound: Systematic review on principles, devices, and clinical applications. J Clin Med 2020;9:460.
3. Insightec. Exablate body. Available from: https://insightec.com/exablate-body/. [Last accessed on 2023 May 24].
4. Profoundmedical. Sonalleve. Available from: https://profoundmedical.com/sonalleve/. [Last accessed on 2023 May 24].
5. Loeve AJ, Al-Issawi J, Fernandez-Gutiérrez F, Langø T, Strehlow J, Haase S, *et al.* Workflow and intervention times of MR-guided focused ultrasound – Predicting the impact of new techniques. J Biomed Inform 2016;60:38-48.
6. Payne A, Chopra R, Ellens N, Chen L, Ghanouni P, Sammet S, *et al.* AAPM task group 241: A medical physicist's guide to MRI-guided focused ultrasound body systems. Med Phys 2021;48:e772-806.
7. Gunderman A, Montayre R, Ranjan A, Chen Y. Review of robot-assisted HIFU therapy. Sensors (Basel) 2023;23:3707.
8. Zaporzan B, Waspe AC, Looi T, Mougenot C, Partanen A, Pichardo S. MatMRI and MatHIFU: Software toolboxes for real-time monitoring and control of MR-guided HIFU. J Ther Ultrasound 2013;1:7.
9. Abdullah B, Subramaniam R, Omar S, Wragg P, Ramli N, Wui A, *et al.* Magnetic resonance-guided focused ultrasound surgery (MRgFUS) treatment for uterine fibroids. Biomed Imaging Interv J 2010;6:e15.
10. Meng Y, Jones RM, Davidson B, Huang Y, Pople CB, Surendrakumar S, *et al.* Technical principles and clinical workflow of transcranial MR-guided focused ultrasound. Stereotact Funct Neurosurg 2021;99:329-42.
11. Vargas-Olivares A, Navarro-Hinojosa O, Pichardo S, Curiel L, Alencastre-Miranda M, *et al*. Image segmentation for the treatment

planning of magnetic resonance-guided high-intensity focused ultrasound (MRgFUS) therapy: A parametric study. Appl Sci 2019;9:1-23.
12. Kociuba J, Łoziński T, Zgliczyńska M, Byrczak M, Vitale SG, Skrzypczak M, *et al.* Adverse events and complications after magnetic resonance-guided focused ultrasound (MRgFUS) therapy in uterine fibroids – A systematic review and future perspectives. Int J Hyperthermia 2023;40:2174274.
13. Anneveldt KJ, Verpalen IM, Nijholt IM, Dijkstra JR, van den Hoed RD, Van't Veer-Ten Kate M, *et al.* Lessons learned during implementation of MR-guided High-intensity focused ultrasound treatment of uterine fibroids. Insights Imaging 2021;12:188.
14. Antoniou A, Georgiou A, Evripidou N, Damianou C. Full coverage path planning algorithm for MRgFUS therapy. Int J Med Robot 2022;18:e2389.
15. Zhou Y, Kargl SG, Hwang JH. The effect of the scanning pathway in high-intensity focused ultrasound therapy on lesion production. Ultrasound Med Biol 2011;37:1457-68.
16. Filippou A, Drakos T, Giannakou M, Evripidou N, Damianou C. Experimental evaluation of the near-field and far-field heating of focused ultrasound using the thermal dose concept. Ultrasonics 2021;116:106513.
17. Ferrer CJ, Bos C, de Senneville BD, Borman P, Stemkens B, Tijssen R, *et al*. A planning strategy for combined motion-assisted/gated MR guided focused ultrasound treatment of the pancreas. Int J Hyperthermia 2019;36:702-11.
18. Schwenke M, Strehlow J, Haase S, Jenne J, Tanner C, Langø T, *et al.* An integrated model-based software for FUS in moving abdominal organs. Int J Hyperthermia 2015;31:240-50.
19. Zhang S, Tang N, Shen G, Wang H, Qiao S. Universal software architecture of magnetic resonance-guided focused ultrasound surgery system and experimental study. J Shanghai Jiaotong Univ 2021;26:471-81.
20. Drakos T, Giannakou M, Menikou G, Filippou A, Evripidou N, Spanoudes K, *et al.* MRI-Guided Focused Ultrasound Robotic System for Preclinical use. J Vet Med Anim Sci 2021;4:1-11.
21. Antoniou A, Georgiou L, Evripidou N, Ioannides C, Damianou C. Challenges regarding MR compatibility of an MRgFUS robotic system. J Magn Reson 2022;344:107317.
22. Antoniou A, Drakos T, Giannakou M, Evripidou N, Georgiou L, Christodoulou T, *et al.* Simple methods to test the accuracy of MRgFUS robotic systems. Int J Med Robot 2021;17:e2287.
23. Antoniou A, Spanoudes K, Damianou C. Treatment of mammary cancer with focused ultrasound: A pilot study in canine and feline patients. Ultrasonics 2023;132:106974.
24. Rieke V, Butts Pauly K. MR thermometry. J Magn Reson Imaging 2008;27:376-90.
25. Sapareto SA, Dewey WC. Thermal dose determination in cancer therapy. Int J Radiat Oncol Biol Phys 1984;10:787-800.
26. Dewhirst MW, Viglianti BL, Lora-Michiels M, Hanson M, Hoopes PJ. Basic principles of thermal dosimetry and thermal thresholds for tissue damage from hyperthermia. Int J Hyperthermia 2003;19:267-94.
27. Yarmolenko PS, Moon EJ, Landon C, Manzoor A, Hochman DW, Viglianti BL, *et al.* Thresholds for thermal damage to normal tissues: An update. Int J Hyperthermia 2011;27:320-43.
28. Bing C, Staruch RM, Tillander M, Köhler MO, Mougenot C, Ylihautala M, *et al.* Drift correction for accurate PRF-shift MR thermometry during mild hyperthermia treatments with MR-HIFU. Int J Hyperthermia 2016;32:673-87.
29. Vykhodtseva N, Sorrentino V, Jolesz FA, Bronson RT, Hynynen K. MRI detection of the thermal effects of focused ultrasound on the brain. Ultrasound Med Biol 2000;26:871-80.
30. Bremer C, Kreft G, Filler T, Reimer P. Accuracy of non-enhanced MRI to monitor histological lesion size during laser-induced interstitial thermotherapy. Eur Radiol 2002;12:237-44.
31. Curiel L, Souchon R, Rouvière O, Gelet A, Chapelon JY. Elastography for the follow-up of high-intensity focused ultrasound prostate cancer treatment: Initial comparison with MRI. Ultrasound Med Biol 2005;31:1461-8.
32. Epaminonda E, Drakos T, Kalogirou C, Theodoulou M, Yiallouras C, Damianou C. MRI guided focused ultrasound robotic system for the treatment of gynaecological tumors. Int J Med Robot 2016;12:46-52.
33. Yiallouras C, Yiannakou M, Menikou G, Damianou C. A multipurpose positioning device for magnetic resonance imaging-guided focused ultrasound surgery. Digit Med 2017;3:138-44.
34. Theraclion | Sonovein ® – Medical Device Treating Varicose Veins. Available from: https://www.theraclion.com/products/sonovein/. [Last accessed on 2023 Dec 05].
35. JC200 Products Chongqing Haifu Medical Technology Co., Ltd. Available from: https://haifumedical.com/html/article/jcc.html. [Last accessed on 2023 Dec 05].
36. Antoniou A, Evripidou N, Panayiotou S, Spanoudes K, Damianou C. Treatment of canine and feline sarcoma using MR-guided focused ultrasound system. J Ultrasound 2022;25:895-904.
37. Chopra R, Curiel L, Staruch R, Morrison L, Hynynen K. An MRI-compatible system for focused ultrasound experiments in small animal models. Med Phys 2009;36:1867-74.
38. Menikou G, Yiallouras C, Yiannakou M, Damianou C. MRI-guided focused ultrasound robotic system for the treatment of bone cancer. Int J Med Robot 2017;13:e1753. [doi: 10.1002/rcs. 1753].
39. Antoniou A, Giannakou M, Evripidou N, Evripidou G, Spanoudes K, Menikou G, *et al.* Robotic system for magnetic resonance guided focused ultrasound ablation of abdominal cancer. Int J Med Robot 2021;17:e2299.
40. Filippou A, Evripidou N, Damianou C. Robotic system for magnetic resonance imaging-guided focused ultrasound treatment of thyroid nodules. Int J Med Robot 2023;19:e2525.
41. Hynynen K, Jones RM. Image-guided ultrasound phased arrays are a disruptive technology for non-invasive therapy. Phys Med Biol 2016;61:R206-48.
42. Haar GT, Coussios C. High intensity focused ultrasound: Physical principles and devices. Int J Hyperthermia 2007;23:89-104.
43. Allen SP, Prada F, Xu Z, Gatesman J, Feng X, Sporkin H, *et al*. A preclinical study of diffusion-weighted MRI contrast as an early indicator of thermal ablation. Magn Reson Med 2021;85:2145-59.
44. Hurwitz MD, Ghanouni P, Kanaev SV, Iozeffi D, Gianfelice D, Fennessy FM, *et al.* Magnetic resonance-guided focused ultrasound for patients with painful bone metastases: Phase III trial results. J Natl Cancer Inst 2014;106:dju082.
45. Lin X, Chen W, Wei F. Technique success, technique efficacy and complications of HIFU ablation for palliation of pain in patients with bone lesions: A meta-analysis of 28 feasibility studies. Ultrasound Med Biol 2021;47:1182-91.
46. Schlesinger D, Benedict S, Diederich C, Gedroyc W, Klibanov A, Larner J. MR-guided focused ultrasound surgery, present and future. Med Phys 2013;40:080901.